BJP British Journal of Pharmacology

DOI:10.1111/bph.12440
www.brjpharmacol.org

RESEARCH PAPER

Andrographolide exerts anti-hepatitis C virus activity by up-regulating haeme oxygenase-1 via the p38 MAPK/Nrf2 pathway in human hepatoma cells

Jin-Ching Lee[1,2], Chin-Kai Tseng[3,4], Kung-Chia Young[3,4,5], Hung-Yu Sun[5], Shainn-Wei Wang[6], Wei-Chun Chen[7], Chun-Kuang Lin[8] and Yu-Hsuan Wu[1]

[1]*Department of Biotechnology, College of Life Science, Kaohsiung Medical University, Kaohsiung, Taiwan,* [2]*Graduate Institute of Natural Products, College of Pharmacy, Kaohsiung Medical University, Kaohsiung, Taiwan,* [3]*Institute of Basic Medical Sciences, College of Medicine, National Cheng Kung University, Tainan, Taiwan,* [4]*Center of Infectious Disease and Signaling Research, College of Medicine, National Cheng Kung University, Tainan, Taiwan,* [5]*Department of Medical Laboratory Science and Biotechnology, College of Medicine, National Cheng Kung University, Tainan, Taiwan,* [6]*Institute of Molecular Medicine, College of Medicine, National Cheng Kung University, Tainan, Taiwan,* [7]*Graduate Institute of Medicine, College of Medicine, Kaohsiung Medical University, Kaohsiung, Taiwan, and* [8]*Doctoral Degree Program in Marine Biotechnology, National Sun Yat-Sen University, Kaohsiung, Taiwan*

Correspondence
Jin-Ching Lee, Department of Biotechnology, College of Life Science, Kaohsiung Medical University, 100, Shih-Chuan 1st Road, San Ming District, 807 Kaohsiung City, Taiwan. E-mail: jclee@kmu.edu.tw

Keywords
HCV; andrographolide; heme oxygenase-1; p38 MAPK; nuclear factor erythroid 2-related factor 2

Received
17 July 2013
Revised
16 September 2013
Accepted
24 September 2013

BACKGROUND AND PURPOSE

This study aimed to evaluate the anti-hepatitis C virus (HCV) activity of andrographolide, a diterpenoid lactone extracted from *Andrographis paniculata*, and to identify the signalling pathway involved in its antiviral action.

EXPERIMENTAL APPROACH

Using HCV replicon and HCVcc infectious systems, we identified anti-HCV activity of andrographolide by measuring protein and RNA levels. A reporter activity assay was used to determine transcriptional regulation of anti-HCV agents. A specific inhibitor and short hairpin RNAs were used to investigate the mechanism responsible for the effect of andrographolide on HCV replication.

KEY RESULTS

In HCV replicon and HCVcc infectious systems, andrographolide time- and dose-dependently suppressed HCV replication. When combined with IFN-α, an inhibitor targeting HCV NS3/4A protease (telaprevir), or NS5B polymerase (PSI-7977), andrographolide exhibited a significant synergistic effect. Andrographolide up-regulated the expression of haeme oxygenase-1 (HO-1), leading to increased amounts of its metabolite biliverdin, which was found to suppress HCV replication by promoting the antiviral IFN responses and inhibiting NS3/4A protease activity. Significantly, these antiviral effects were attenuated by an HO-1-specific inhibitor or HO-1 gene knockdown, indicating that HO-1 contributed to the anti-HCV activity of andrographolide. Andrographolide activated p38 MAPK phosphorylation, which stimulated nuclear factor erythroid 2-related factor 2 (Nrf2)–mediated HO-1 expression, and this was found to be associated with its anti-HCV activity.

CONCLUSIONS AND IMPLICATIONS

Our results demonstrate that andrographolide has the potential to control HCV replication and suggest that targeting the Nrf2–HO-1 signalling pathway might be a promising strategy for drug development.

Abbreviations

ARE, antioxidant response element; BVR, biliverdin reductase; CI, combination index; HCC, hepatocellular carcinoma; HCV, hepatitis C virus; HCVcc, cell culture-derived infectious HCV particles; HO-1, haeme oxygenase 1; ISGs, IFN-stimulated genes; OAS, 2′-5′-oligoadenylate synthetase; ISRE, IFN-stimulated response element; Keap1, Klech-like ECH-associated protein 1; Nrf2, nuclear factor erythroid 2-related factor 2; PEG-IFN-α, pegylated IFN-α; qRT-PCR, quantitative real-time RT-PCR; SEAP, secreted alkaline phosphatase; SnPP, tin protoporphyrin IX dichloride

Introduction

Hepatitis C virus (HCV) is an enveloped virus belonging to the *Hepacivirus* genus in the Flaviviridae family. It has a 9.6 kb genome encoding a single polyprotein that is cleaved by cellular and viral proteases into 10 separate proteins, including four structural proteins (C, E1, E2 and p7) and six non-structural proteins (NS2, NS3, NS4A, NS4B, NS5A and NS5B) (Brass *et al.*, 2006). HCV infects more than 170 million people worldwide and is the main aetiological factor in the development of liver fibrosis, cirrhosis, portal hypertension, hepatic failure and hepatocellular carcinoma (HCC; Alter, 2007). There is no available vaccine to prevent HCV infection. The current HCV therapy, a combination of pegylated IFN-α (PEG-IFN-α) plus ribavirin, is effective in only approximately 50% of cases and provokes severe side effects, including depression, fatigue, flu-like symptoms and haemolytic anaemia (Ghany *et al.*, 2009; Schoggins *et al.*, 2011). At present, two NS3/4A protease inhibitors approved by the US Food and Drug Administration (FDA), telaprevir (Incivek; Vertex Pharmaceuticals Incorporated, Cambridge, MA, USA) and boceprevir (Victrelis; Merck Corporate, Whitehouse Station, NJ, USA), in combination with PEG-IFN-α and ribavirin exhibited higher sustained virological response rates for the treatment of genotype 1 chronic hepatitis C (Kiser *et al.*, 2012). However, drug-resistant variants and psychiatric responses to both inhibitors were observed in clinical studies (Susser *et al.*, 2009; Sarrazin and Zeuzem, 2010), which may reduce the efficacy and usefulness of current HCV triple therapies and hinder the development of IFN-free therapy. There is, thus, a need to develop alternative anti-HCV agents with higher efficacy and more favourable side-effect profiles for anti-HCV therapeutics. In this study, we used an HCV subgenomic replicon system to screen many natural products and finally identified a potent agent, andrographolide (Figure 1A), as having anti-HCV activity.

Andrographis paniculata (Burm. f) Nees, a member of the Acanthaceae family, is a medicinal plant used for a long time in India, Japan, China, Korea and other Asian countries to treat a range of illnesses, including bacterial infections, inflammations and high BP (Coon and Ernst, 2004; Sule *et al.*, 2012). Andrographolide is the most abundant diterpene lactone in the leaves and stems of *A. paniculata* and is a dietary supplement widely used in herbal medicine because of its diverse biological activities, which include anti-inflammatory, anti-metastasis, anti-angiogenesis, anti-proliferation, neuroprotective and hepatoprotective effects (Chan *et al.*, 2010; Maiti *et al.*, 2010). In addition, andrographolide exhibits antiviral activity against the human immunodeficiency virus (Uttekar *et al.*, 2012), herpes simplex virus 1 (Seubsasana *et al.*, 2011), influenza virus (Chen *et al.*, 2009) and Epstein–Barr virus (Lin *et al.*, 2008) via different mechanisms. To date, no investigations of the anti-HCV activity of andrographolide have been reported. In the present study, we evaluated the effects of andrographolide on HCV activity and investigated the mechanism by which andrographolide blocks HCV replication. Andrographolide was recently shown to promote gene expression of haeme oxygenase-1 (HO-1) via activation of nuclear factor erythroid 2-related factor 2 (Nrf2) and to inhibit cancer cell migration (Yu *et al.*, 2010; Chao *et al.*, 2013). The HO-1 metabolite biliverdin was recently shown to possess anti-HCV activity (Lehmann *et al.*, 2010; Zhu *et al.*, 2010). Therefore, the possibility that the Nrf2-mediated HO-1 signalling pathway is involved in the anti-HCV activity of andrographolide was investigated in this study.

HO-1 is the rate-limiting enzyme in the production of Fe^{2+}, carbon monoxide and biliverdin through haeme catabolism (Maines, 2005). Biliverdin is subsequently catabolized into bilirubin by biliverdin reductase (BVR). HO-1 is an inducible enzyme showing a protective effect against inflammatory processes and oxidative tissue damage induced by exposure to multiple stimuli such as viral and bacterial products, including LPSs, cytokines, oncogenes, mitogens and growth factors (Farombi and Surh, 2006; Paine *et al.*, 2010). Among the intracellular factors capable of regulating HO-1, Nrf2 is a major activator of HO-1 expression. It functions by binding to the antioxidant response element (ARE) in the HO-1 promoter region following binding to small Maf protein. In contrast, Bach1 is an antagonist of Nrf2 that suppresses HO-1 expression by competitive binding to ARE (Shan *et al.*, 2006). Under physiological/basal conditions, Nrf2 undergoes proteasomal degradation by binding to its repressor Kelch-like ECH-associated protein 1 (Keap1) in the cytosol. Under stress-inducing conditions, Nrf2 dissociates from Keap1 and subsequently translocates to the nucleus, where it binds to ARE for activation of phase II detoxifying enzymes including HO-1, NADPH, quinone oxidoreductase-1, glutathione S-transferase and glutamine-cysteine ligase, which play an important role in protecting against carcinogenesis (Liang *et al.*, 2013). MAPK molecules, including the p38 MAPK, ERK1/2 and JNK, up-regulate the expression of Nrf2/ARE-dependent HO-1, and this pathway is involved in the anti-inflammatory and antioxidative effects of several compounds (Paine *et al.*, 2010). Hence, we investigated the effect of andrographolide on MAPKs signalling with regard to its anti-HCV activity.

Methods

Cell culture and reagents

Human hepatoma cells (Huh-7) and Huh-7 cells containing HCV subgenomic RNA replicon cells (Ava5) (Blight *et al.*,

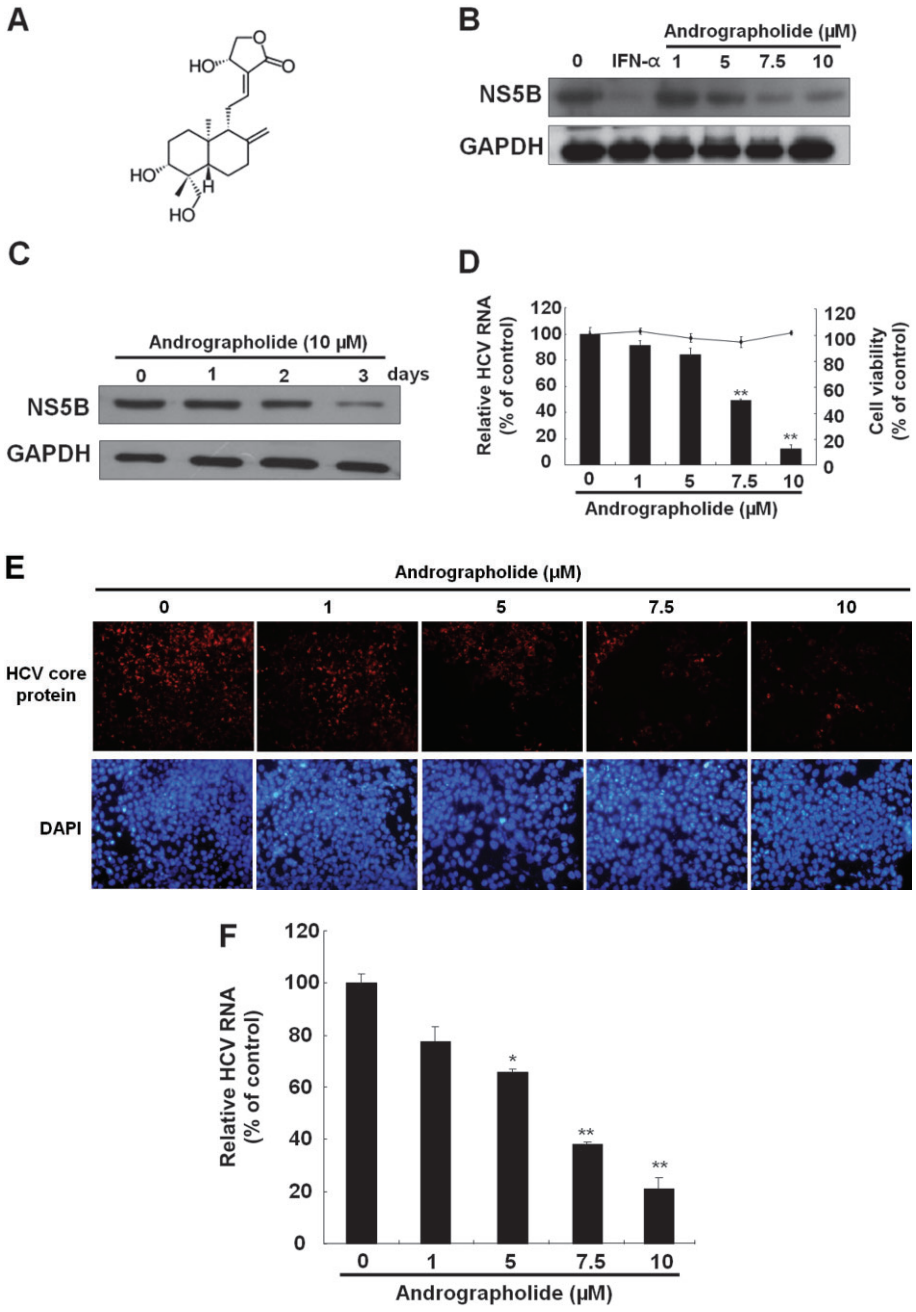

Figure 1

Andrographolide inhibits HCV replication. (A) Structure of andrographolide. The molecular formula is $C_{20}H_{30}O_5$. (B, C) Reduction of HCV protein synthesis by andrographolide in a (B) concentration- and (C) time-dependent manner. Ava5 cells were treated with andrographolide at different concentrations (0–10 μM) for 3 days or for different time periods (1–3 days) with 10 μM andrographolide. IFN-α treatment served as a positive control. Protein synthesis was evaluated by Western blotting with anti-HCV NS5B antibody. Equal loading of cell lysates was confirmed by probing the same blot with anti-GAPDH antibody. (D) Reduction of HCV RNA replication by andrographolide in Ava5 cells. qRT-PCR was performed to quantify HCV RNA levels in the andrographolide-treated Ava5 cells after 3 days of incubation. The HCV RNA level was normalized against the cellular *gapdh* mRNA level and is presented as the percentage change relative to the andrographolide-untreated control. Cellular toxicity was evaluated by the MTS assay after incubation of cells with andrographolide for 3 days and is presented as the percentage change relative to the andrographolide-untreated control. (E, F) Concentration-dependent inhibition of HCVcc protein expression (E) and RNA replication (F) by andrographolide. The HCVcc-infected Huh-7 cells were treated with andrographolide at different concentrations (0–10 μM). On day 9 after infection, the HCV core-positive cells were detected by the immunofluorescence assay using anti-HCV core antibody. The total cells were visualized using DAPI nucleus stain. At 3 days after infection, HCV RNA levels and cell viability were assayed by qRT-PCR and MTS respectively. Results are represented as means ± SD (error bar) of three independent experiments. $^*P < 0.05$, $^{**}P < 0.01$.

2000) were cultured in DMEM with 10% heat-inactivated FBS, 1% antibiotic–antimycotic, 1% non-essential amino acids and 1 mg·mL^{-1} G418. The IFN-α-2a (Roferon©-A) was purchased from Roche Ltd. (Basel, Switzerland). Andrographolide, an HO-1-specific inhibitor [tin protoporphyrin IX dichloride (SnPP)], and MAPK-specific inhibitors (SP600125, SB203580 and PD98059) were purchased from Sigma (St. Louis, MO, USA). PSI-7977 was purchased from Shanghai Haoyuan Chemexpress Co., Ltd. (Shanghai, China). Telaprevir was purchased from Legend Stat International Co., Ltd. (Omdurman, Sudan). The final concentration of DMSO in all reactions was maintained at 0.1%.

Plasmid construction

pHO-1-Luc (Hill-Kapturczak *et al.*, 2003) and p2xARE-Luc (Liao *et al.*, 2008) vectors were used to measure the transcriptional activity of HO-1 and Nrf2 respectively. pISRE-Luc, a reporter vector containing firefly luciferase under the control of an IFN-stimulated response element (ISRE), was used to measure IFN response-dependent transcriptional activity (Stratagene, Agilent Technologies, La Jolla, CA, USA). HO-1 (NM_002133), Nrf2 (NM_006164) and eGFP short hairpin RNA (shRNA) were purchased from the National RNAi Core Facility, Institute of Molecular Biology/Genomic Research Center, Academia Sinica, Taipei, Taiwan. All cloned DNA fragments were verified by DNA sequencing.

Western blotting

Western blotting was performed as described previously (Lee *et al.*, 2010). Equal amounts of cell lysates were resolved by SDS-PAGE, followed by transfer to a nitrocellulose membrane. The membranes were probed with anti-HCV NS5B (1:5000; Abcam, Cambridge, MA, USA), anti-HO-1 (1:3000; Abcam), anti-BVR antibody (1:1000; Abcam), anti-Nrf2 (1:3000; GeneTex, Irvine, CA, USA), anti-Keap1 (1:1000; GeneTex), anti-Bach1 (1:1000; Abcam), anti-phospho-ERK1/2 (1:1000; Cell Signaling Technology, Inc., Danvers, MA, USA), anti-phospho-p38 (1:1000; Cell Signaling), anti-phospho-JNK (1:1000; Cell Signaling), anti- ERK1/2 (1:1000; Cell Signaling), anti-p38 (1:1000; Cell Signaling), anti-JNK (1:1000; Cell Signaling) or anti-lamin B1 (1:1000; GeneTex) antibody. A loading control was determined using anti-GAPDH antibody (1:10 000; GeneTex). The signal was detected using an ECL detection kit (PerkinElmer, Shelton, CT, USA).

Quantification of HCV RNA and cellular mRNAs

RNA isolation and quantitative real-time RT-PCR (qRT-PCR) were performed as described previously (Chen *et al.*, 2013b). Relative mRNA levels were obtained by normalization against the cellular endogenous *gapdh* gene. Primers used in the study are listed in Table 1.

Preparation of HCVcc stock and evaluation of antiviral activity

Huh-7.5 cells stably expressing the pEF/JFH1-Rz/N plasmid were grown to produce cell culture-derived infectious HCV particles (HCVcc), and the conditional medium was collected to harvest viral particles according to the protocol described previously (Kato *et al.*, 2007). Fifty percent tissue culture infective dose of virus was determined by the immunofluorescence assay with specific antibody against HCV core protein (Abcam). For the antiviral activity assay, the Huh-7 cells were seeded at a density of 4×10^4 cells per well in a 24-well plate and infected with 100 μL HCVcc at a multiplicity of infection of 0.1 for 6 h followed by incubation with various concentrations of andrographolide with or without SnPP for an additional 3 or 9 days. Then, qRT-PCR or immunostaining was used to determine anti-HCV activity.

Table 1
Oligonucleotide sequences for real-time RT-PCR

Oligonucleotide name	Sequence 5′-3′
5′ NS5B	5′-GGA AACCAAGCTGCCCATCA
3′ NS5B	5′-CCTCCACGGATAGAAGTTTA
5′ GAPDH	5′-GTCTTCACCACCATGGAGAA
3′ GAPDH	5′-ATGGCATGGACTGTGGTCAT
5′ OAS1	5′-CAAGCTTAAGAGCCTCATCC
3′ OAS1	5′-TGGGCTGTGTTGAAATGTGT
5′ OAS2	5′-ACAGCTGAAAGCCTTTTGGA
3′ OAS2	5′-GCATTAAAGGCAGGA AGCAC
5′ OAS3	5′-CACTGACATCCCAGACGATG
3′ OAS3	5′-GATCAGGCTCTTCAGCTTGG
5′ PKR	5′-ATGATGGAAAGCGAACAAGG
3′ PKR	5′-GAGATGATGCCATCCCGTAG
5′ IFN-α-2	5′-GCA AGT CAA GCT GCT CTG TG
3′ IFN-α-2	5′-GAT GGT TTC AGC CTT TTG GA
5′ IFN-α-5	5′-AGTTTGATGGCAACCAGTTC
3′ IFN-α-5	5′-TCAGAGGAGTGTCTTCCACT
5′ IFN-α-17	5′-AGG AGT TTG ATG GCA ACC AG
3′ IFN-α-17	5′-CAT CAG GGG AGT CTC TTC CA

Immunofluorescence assay for HCV infection

For the immunofluorescence assay, the cells were fixed and permeabilized with methanol and 0.2% Triton X-100 (Sigma). After being blocked with 4% BSA, the HCV core protein was reacted with anti-core antibody and visualized by goat anti-mouse Alexa-592 (Invitrogen, Carlsbad, CA, USA) under fluorescence microscopy. The nucleus was stained with DAPI (Sigma).

Cytotoxicity assay

Cell viability was determined using a standard MTS assay (CellTiter 96® AQ_{ueous} One Solution Cell Proliferation Assay System; Promega, Madison, WI, USA), according to the manufacturer's instructions. In brief, Huh-7 or Ava5 cells were seeded in a 96-well plate at a density of 5×10^3 cells per well and supplemented with various concentrations of andrographolide for 3 days. Colour intensity was detected at 490 nm using a 550 Bio-Rad plate reader (Hertfordshire, UK).

Transfection and luciferase activity assay

To evaluate the effect of andrographolide on the transcriptional regulation of HO-1 or the response to Nrf2 or IFN,

the promoter-driven firefly luciferase plasmid, pHO-1-Luc, p2xARE-Luc or pISRE-Luc was transfected into Ava5 cells using the T-Pro™ transfection reagent (Ji-Feng Biotechnology Co., Ltd., Taipei, Taiwan), according to the manufacturer's instructions. Then, the transfected cells were treated with andrographolide at various concentrations for 3 days. To evaluate the role of HO-1 and Nrf2 in the effect of andrographolide on HCV replication, the HO-1 or Nrf2 shRNA expression vector (pHO-1-shRNA and pNrf2-shRNA; 0.5 or 1.0 μg, respectively) was transfected into the Ava5 cells, followed by incubation in10 μM andrographolide with or without SnPP for 3 days. Each transfection complex contained 0.1 μg secreted alkaline phosphatase (SEAP) expression vector (pSEAP) as a transfection control for normalization against luciferase activity. Cell lysates were prepared for the luciferase activity assay and Western blotting using the Bright-Glo Luciferase Assay System (Promega) and specific antibodies respectively. The supernatants were harvested for the SEAP activity assay using the Phospha-Light Assay Kit (Tropix, Foster City, CA, USA). For each experiment, luciferase activity was calculated by normalizing to the SEAP activity.

NS3/4A activity assay

The cell-based NS3/4A activity assay was performed as described previously (Chen *et al.*, 2013b). In brief, the NS3/4A protease reporter vector pEG(DEΔ4AB)SEAP and NS3/4A expression vector pNS3/4A were co-transfected into Huh-7 cells, followed by incubation in the presence of andrographolide with or without SnPP for 3 days. Supernatants were harvested for the SEAP activity assay using the Phospha-Light Assay Kit (Tropix). Each transfection mixture contained 0.1 μg firefly luciferase expression vector (pFLuc) as a transfection control for normalization against the SEAP activity.

BVR activity assay

Ava5 cells were seeded in a 10 cm tissue culture plate at a density of 2×10^6 cells per plate and treated with increasing concentrations of andrographolide for 3 days. The cell lysates were subjected to measurement of BVR activity using a BVR assay kit (Sigma) according to the manufacturer's instructions. Activity was calculated from a standard curve generated by a BVR positive control solution (Sigma). Absorbance was detected at 450 nm using an Epoch microplate spectrophotometer (BioTek Instruments, Inc., Winooski, VT, USA).

Quantification of intracellular bilirubin

Measurement of the intracellular bilirubin level was performed as described previously (Chen *et al.*, 2013b). In brief, cells were seeded in 6-well plates at a density of 4×10^5 cells per plate and treated with andrographolide at various concentrations for 3 days. Cell lysates were harvested to measure bilirubin concentration using a MeDiPro direct bilirubin test kit (Formosa Biomedical Technology Corp., Taipei, Taiwan) and calibrator for automated systems (Roche Diagnostics Ltd., South San Francisco, CA, USA). Absorbance was detected at 546 and 660 nm using an Epoch microplate spectrophotometer (BioTek Instruments, Inc.).

Quantification of extracellular IFN-α

Cells were seeded in 24-well plates at a density of 4×10^4 cells per well and treated with various concentrations of andrographolide in the presence or absence of SnPP for 3 days. Cell culture medium was harvested to measure IFN-α concentration using a Human IFN-α ELISA Kit (USCN Life Science Inc., Wuhan, China) according to the manufacturer's protocol. Absorbance was detected at 450 nm using an Epoch microplate spectrophotometer (BioTek Instruments, Inc.).

Nuclear fraction preparation

Ava5 cells were seeded in a 10 cm dish and treated with increasing concentrations of andrographolide for 3 days. The cells were then collected for preparation of a nuclear fraction as described previously (Chen *et al.*, 2013b).

Assessment of effect of andrographolide on the stimulation of MAPK signalling pathway

For detection of phosphorylation level of MAPKs, cells were seeded in 6-well plates at a density of 3×10^5 cells per well and treated with 10 μM andrographolide for different time periods (0, 15, 30, 45, 60, 120 min). Total lysates were prepared for Western blot analysis with specific antibodies against anti-phospho-ERK1/2, anti-phospho-p38, anti-phospho-JNK, anti- ERK1/2, anti-p38 or anti-JNK. To determine the MAPK that mediated the HO-1 stimulation involved in the anti-HCV activity of andrographolide, Ava5 or p2xARE-Luc-transfected Ava5 cells were treated with 10 μM andrographolide in the presence of inhibitors of either ERK (15 μM PD98059), p38 (15 μM SB203580) or JNK (30 μM SP600125) for 3 days. Total lysates were prepared for Western blot analysis with specific antibodies or luciferase activity assay using the Bright-Glo Luciferase Assay System (Promega).

Analysis of drug synergism

Ava5 cells were treated with serially diluted andrographolide (0, 1.25, 2.5, 5.0, 7.5 and 10.0 μM) in combination with serially diluted IFN-α (7.5, 15, 30 and 60 $U \cdot mL^{-1}$), PSI-7977 (0.75, 1.5, 3.0 and 6.0 μM) or telaprevir (0.075, 0.15, 0.3 and 0.6 μM). After 3 days of incubation, HCV RNA levels were determined by qRT-PCR. Multiple drug combination data were analysed using CalcuSyn2™ software (Biosoft, Cambridge, UK) based on the method of Chou and Talalay (1984), which compares single and multiple drug dose effects and determines the combination index (CI) value. The effect of a multiple drug combination is presented as antagonism (CI > 1), additivity (CI = 1) or synergism (CI < 1).

Statistical analysis

All data are presented as means ± SD of triplicate experiments. Statistical analysis was performed using Student's *t*-test. A significant difference was considered if $^*P < 0.05$ or $^{**}P < 0.01$.

Results

Andrographolide inhibits the protein synthesis, RNA replication and infection of HCV

To examine the anti-HCV activity of andrographolide (Figure 1A), we first treated Ava5 cells (Blight *et al.*, 2000),

which are Huh-7 cells containing HCV subgenomic RNA replicon, with andrographolide at increasing concentrations (0–10 μM) for 3 days or at a concentration of 10 μM for various incubation times (1–3 days); treatment with 100 U·mL^{-1} IFN-α served as a positive control of anti-HCV activity. Western blotting and qRT-PCR analysis were then performed to evaluate the inhibitory effect of andrographolide on HCV protein synthesis and RNA replication respectively. Simultaneously, a MTS assay was performed under the same experimental conditions to rule out the possibility that any antiviral activity observed is as a result of a cytotoxic effect of andrographolide. The results indicated that the amount of HCV NS5B protein was proportionally reduced by andrographolide treatment with increasing concentrations or incubation times (Figure 1B and C). Similarly, andrographolide significantly reduced HCV RNA levels with an EC_{50} value of 6.0 ± 0.5 μM and was not cytotoxic at effective antiviral concentrations (Figure 1D). Next, we performed an HCVcc infectious assay to confirm the anti-HCV activity of andrographolide by immunostaining and qRT-PCR. The results revealed that andrographolide concentration- dependently reduced HCV core protein expression in HCVcc-infected Huh-7 cells compared with andrographolide-untreated cells with HCVcc infection (Figure 1E). As expected, andrographolide effectively reduced HCV RNA levels in a concentration-dependent manner, with an EC_{50} value of 5.1 ± 0.7 μM (Figure 1F).

Andrographolide elevates HO-1 mRNA and protein levels in HCV replicon cells

Andrographolide has been shown to up-regulate Nrf2-dependent HO-1 expression and prevent oxidative damage (Guan *et al.*, 2013), and to inhibit TNF-α-induced expression of intercellular adhesion molecule (Yu *et al.*, 2010). To determine whether andrographolide affects the expression of HO-1 gene in HCV replicon cells, we initially tested the effect of andrographolide on HO-1 gene transcription using a transient HO-1 promoter-based reporter assay. The reporter construct, pHO-1-Luc, contains a firefly luciferase gene driven by the HO-1 promoter. Ava5 cells were transfected with the pHO-1-Luc reporter plasmid and then treated with increasing concentrations of andrographolide for 3 days, with pHO-1-Luc-transfected parental Huh-7 cells without andrographolide treatment serving as a reference for the basal level of HO-1 expression. The results showed that viral proteins dramatically inhibited HO-1 promoter-deriving luciferase activity in the Ava5 cells compared with the basal HO-1 promoter activity in the Huh-7 cells. Andrographolide significantly stimulated the HO-1 promoter activity in these HCV-treated cells in a concentration-dependent manner (Figure 2A). Next, the expression of HO-1 RNA and protein levels were evaluated by qRT-PCR and Western blotting respectively. As expected, andrographolide also concentration-dependently increased HO-1 RNA and protein levels in these HCV replicon cells (Figure 2B and C).

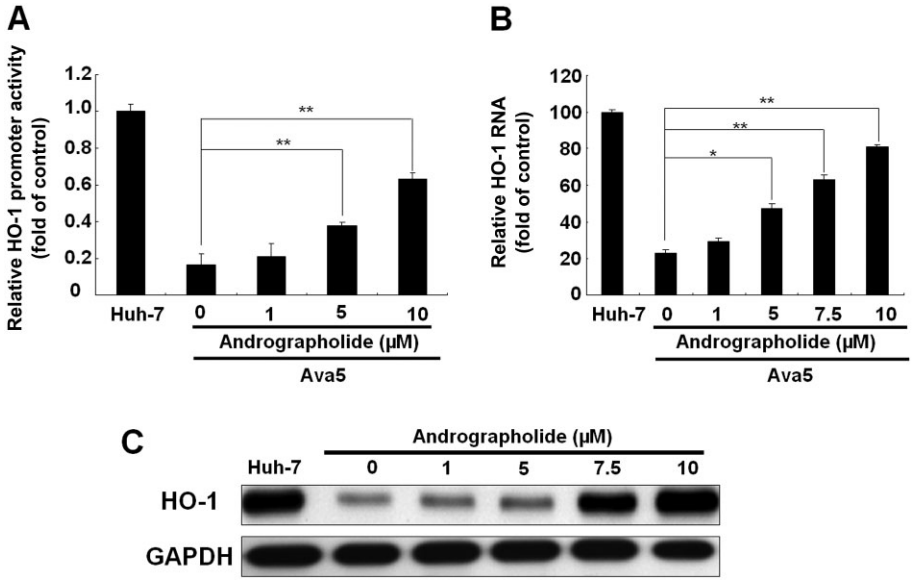

Figure 2

Andrographolide induces HO-1 expression. (A–C) Induction of HO-1 promoter activity (A), HO-1 mRNA transcription (B) and HO-1 protein synthesis (C) by andrographolide in Ava5 cells. The HO-1 promoter-linked firefly luciferase (FLuc) vector, pHO-1-Luc, was transiently transfected into Ava5 cells. Each transfection mixture contained 0.1 μg pSEAP reporter plasmid as a control of transfection efficiency. The transfected cells were then treated with andrographolide at different concentrations (0–10 μM) for 3 days. The HO-1 promoter activity was assayed for luciferase activity and presented as fold activation relative to a parental Huh-7 cell control (defined as 1) following normalization against SEAP activity. The HO-1 RNA level was normalized against the cellular *gapdh* mRNA level and presented as the percentage change relative to parental Huh-7 cells (defined as 100%). Protein synthesis was detected by Western blotting with anti-HO-1 antibody. Equal loading of cell lysates was confirmed by probing the same blot with anti-GAPDH antibody. The experiments were performed in triplicate, and error bars indicate mean ± SD. *$P < 0.05$, **$P < 0.01$.

Andrographolide enhances the production of the HO-1 product biliverdin for activating antiviral IFN response and suppressing HCV NS3/4A protease activity

Studies by Lehmann *et al*. (2010) have demonstrated that the HO-1 product biliverdin interferes with HCV replication by increasing the antiviral IFN response. To determine whether andrographolide, by increasing the activity of HO-1, has the same effect against HCV replication in our study (Figure 2), we first measured the amount of bilirubin, the biliverdin metabolite, formed after andrographolide treatment at increasing concentrations for 3 days, with measurement of parental Huh-7 cells providing the basal level of bilirubin. As shown in Figure 3A, andrographolide significantly increased the bilirubin levels in HCV-treated Ava5 cells. Biliverdin reductase (BVR) controls the conversion of biliverdin to bilirubin (Kravets *et al*., 2004). We next examined whether andrographolide increases the level of bilirubin by stimulating BVR activity. As shown in Figure 3B, no significant stimulation of BVR activity was observed following andrographolide treatment. Similar results were observed for BVR RNA (Figure 3C) and protein (Figure 3D) levels under identical conditions. Because the conversion of biliverdin to bilirubin is proportional, we concluded that the amount of biliverdin was enhanced by andrographolide treatment because of the increase in HO-1 (Figure 2). To investigate whether andrographolide-enhanced biliverdin levels were able to activate a cellular antiviral IFN response, the Ava5 cells were transfected with the pISRE-luciferase reporter plasmid carrying ISRE-driven firefly luciferase and then cultured with andrographolide, at increasing concentrations for 3 days. As shown in Figure 4A (panel a), andrographolide significantly increased ISRE promoter activities, as determined by the measurement of luciferase activity. In contrast, treatment with the HO-1-specific inhibitor SnPP concentration- dependently attenuated the increased ISRE promoter activity induced by andrographolide [Figure 4A (panel b)]. Similar results were observed for IFN-α-2, -α-5 and -α-17 mRNA expression in andrographolide-treated Ava5 cells with or without SnPP [Figure 4A (panels c and d)]. As expected, andrographolide treatment concentration-dependently increased the IFN-α protein level in the supernatant, and this effect was attenuated by the addition of SnPP (Figure 4B). To confirm further that the antiviral IFN pathway was stimulated by andrographolide, the expression of critical IFN-stimulated genes (ISGs) against viral infection, including 2′-5′-oligoadenylate synthetase 1 (OAS1), OAS2, OAS3, PKR

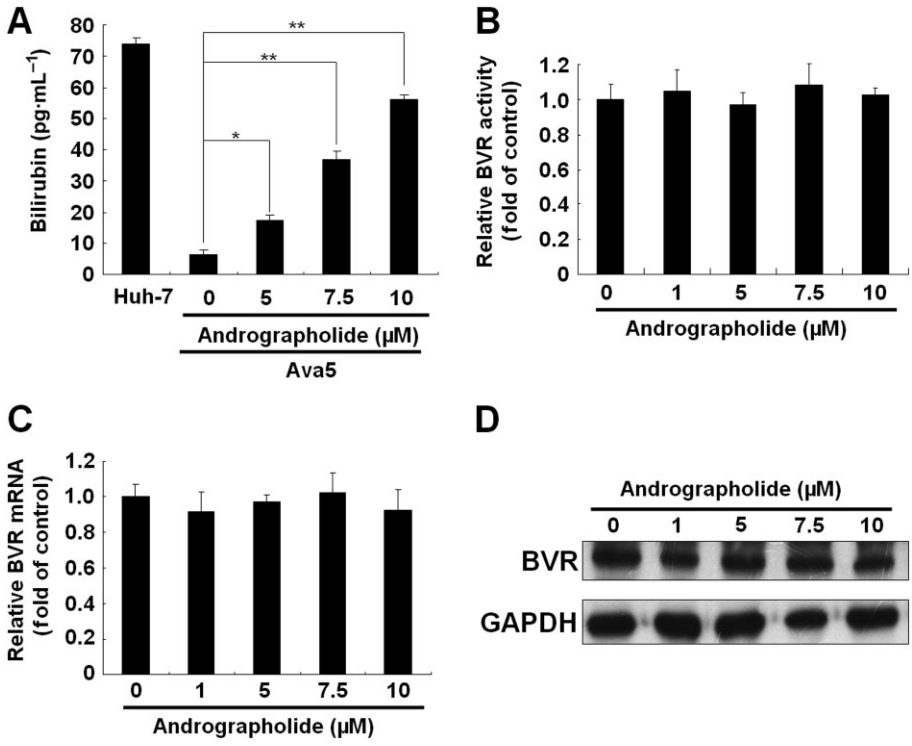

Figure 3

Andrographolide induces bilirubin production. (A–D) Effect of andrographolide on bilirubin concentration (A), BVR enzymatic activity (B), BVR mRNA transcription (C) and BVR protein synthesis (D). Ava5 cells were treated with the indicated concentrations of andrographolide (0–10 μM) for 3 days. The amount of bilirubin was measured using the MeDiPro direct bilirubin test kit and calibrator for automated systems. The basal amount of bilirubin was shown in parental Huh-7 cells. The total cell lysates were subjected to the BVR activity assay and Western blotting with anti-BVR and anti-GAPDH (loading control) antibodies. BVR activity is presented as fold change relative to the andrographolide-untreated control (defined as 1). The HCV RNA level was analysed by qRT-PCR, which was normalized against the cellular *gapdh* mRNA level and presented as fold change relative to the andrographolide-untreated control (defined as 1). The experiments were performed in triplicate, and error bars indicate mean ± SD. *$P < 0.05$, **$P < 0.01$.

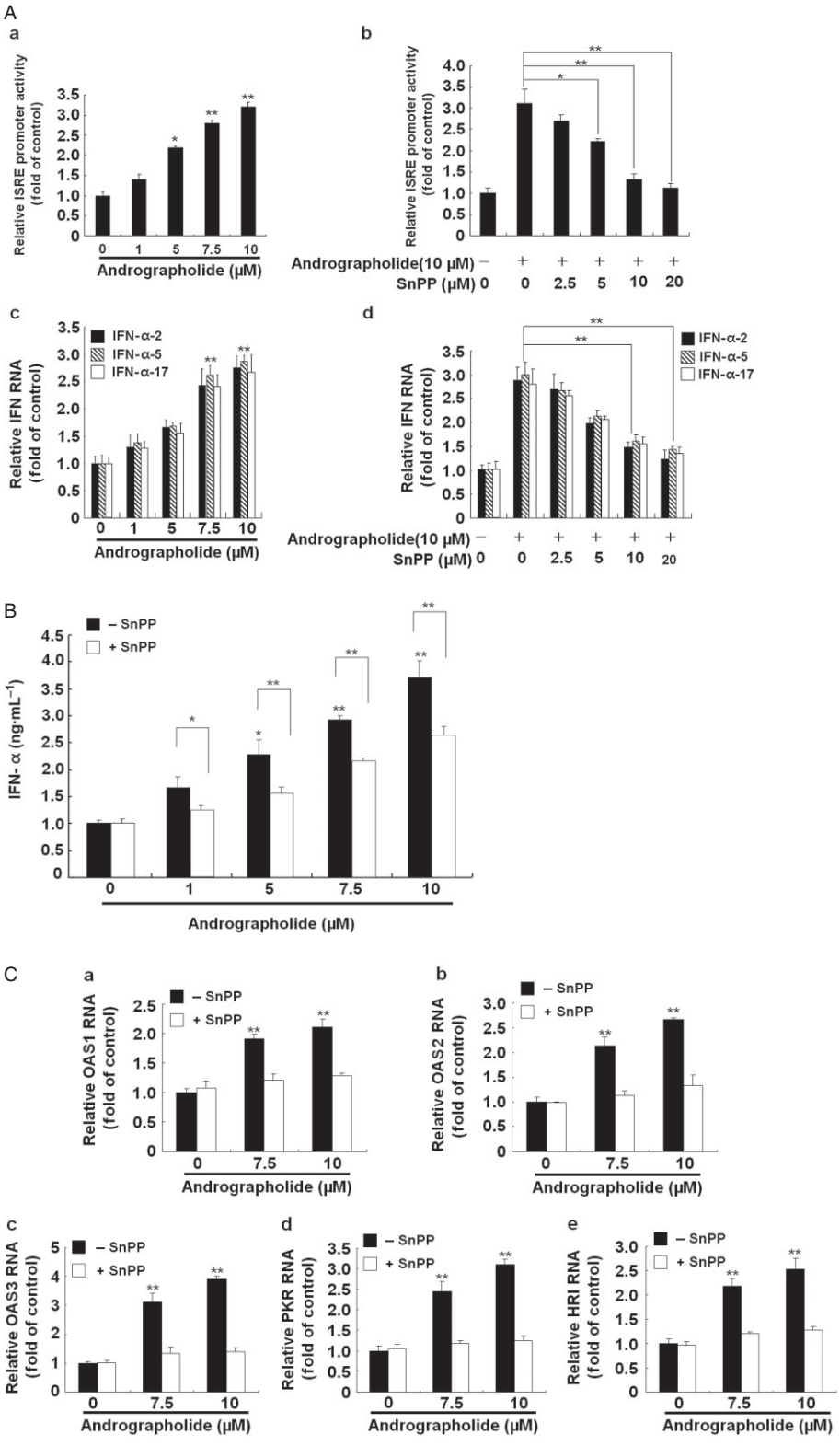
A
a
Relative ISRE promoter activity (fold of control)
Andrographolide (μM)
b
Relative ISRE promoter activity (fold of control)
Andrographolide(10 μM)
SnPP (μM)
c
IFN-α-2
IFN-α-5
IFN-α-17
Relative IFN RNA (fold of control)
Andrographolide (μM)
d
Relative IFN RNA (fold of control)
Andrographolide(10 μM)
SnPP (μM)
B
– SnPP
+ SnPP
IFN-α (ng·mL⁻¹)
Andrographolide (μM)
C
a
Relative OAS1 RNA (fold of control)
b
Relative OAS2 RNA (fold of control)
c
Relative OAS3 RNA (fold of control)
d
Relative PKR RNA (fold of control)
e
Relative HRI RNA (fold of control)

Figure 4

Andrographolide induces antiviral IFN responses via HO-1 induction. (A, panels a–d) Induction of ISRE activity (a) and gene expression of IFN-α-2, IFN-α-5 and IFN-α-17 (c) by andrographolide and attenuation of this effect by the HO-1-specific inhibitor SnPP (b and d). (B) Induction of IFN-α protein level by andrographolide and attenuation of this stimulant effect by SnPP. (C, panels a–e) Induction of IFN-mediated gene expression by andrographolide and suppression of this effect by SnPP. Ava5 cells or pISRE-Luc-transfected Ava5 cells were incubated with andrographolide alone at the indicated concentrations (0–10 μM) or coincubated with increasing concentrations of SnPP (0–20 μM) and 10 μM andrographolide for 3 days. The ISRE promoter activity was assayed for luciferase activity and was presented as fold activation relative to andrographolide/SnPP-untreated cells (defined as 1). The protein level of extracellular IFN-α was measured by ELISA. The mRNA levels of IFN-α-2, IFN-α-5, IFN-α-17, OAS1, OAS2, OAS3, PKR or haeme-regulated inhibitor were measured by qRT-PCR and normalized against the cellular *gapdh* mRNA level and presented as fold change relative to the andrographolide/SnPP-untreated control (defined as 1). The experiments were performed in triplicate, and error bars indicate mean ± SD. $*P < 0.05$, $**P < 0.01$.

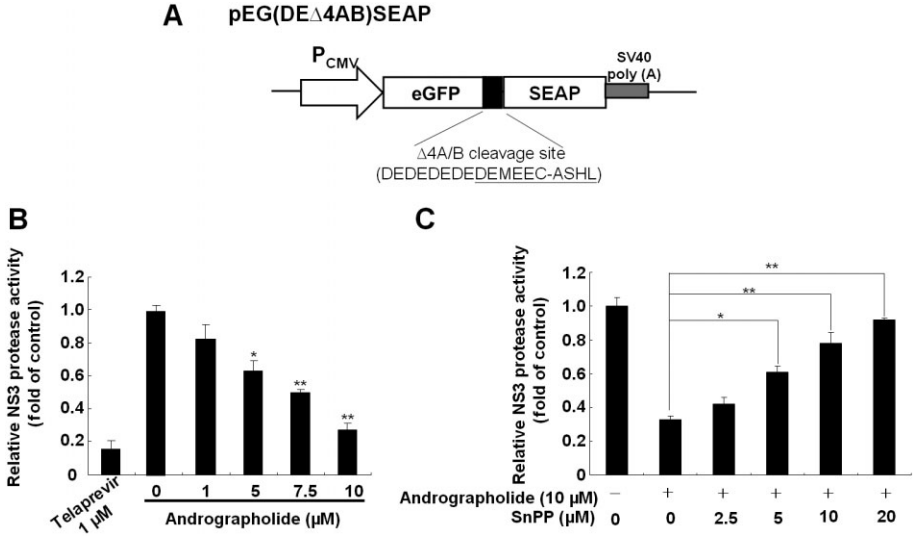

Figure 5

Andrographolide inhibits HCV NS3/4A protease activity via HO-1 induction. (A) Schematic diagram of the NS3/4A response reporter vector including the HCV cleavage site flanked by *egfp* and *seap* genes, named as pEG(DEΔ4AB)SEAP. (B) Andrographolide inhibited NS3/4A protease activity in a concentration-dependent manner. (C) Restoration of andrographolide-reduced NS3/4A protease activity by the HO-1-specific inhibitor SnPP. The pEG(DEΔ4AB)SEAP vector and the NS3/4A expression vector pNS3/4A were transiently co-transfected into Huh-7 cells. Each transfection mixture contained 0.1 μg pFLuc reporter plasmid as a control of transfection efficiency. The transfected cells were then treated with andrographolide alone at different concentrations (0–10 μM) or co-treated with increasing concentrations of SnPP (0–20 μM) and 10 μM andrographolide for 3 days. Telaprevir treatment served as the positive control. The NS3/4A protease activity was determined by SEAP activity following normalization against luciferase activity and presented as fold change relative to the andrographolide/SnPP-untreated control (defined as 1). The experiments were performed in triplicate, and error bars indicate mean ± SD. $*P < 0.05$, $**P < 0.01$.

and haeme-regulated inhibitor (Onomoto *et al.*, 2012), was examined by using qRT-PCR. As shown in Figure 4C (panels a–e), andrographolide significantly increased ISG expression at concentrations of 7.5 and 10.0 μM , and SnPP treatment concentration-dependently attenuated this effect of andrographolide on ISG expression. Zhu *et al.* (2010) recently proposed another anti-HCV mechanism of biliverdin; it acts by inhibiting HCV NS3/4A protease activity. We performed a cell-based reporter assay to examine the possibility of andrographolide targeting HCV NS3/4A protease activity through biliverdin production. The reporter plasmid pEG(DE4AB)SEAP is illustrated in Figure 5A, with SEAP activity in the culture medium reflecting NS3/4A protease activity in the cell-based assay (Lee *et al.*, 2003; Chen *et al.*, 2013b). Huh-7 cells were co-transfected with pEG(DE4AB)SEAP and pNS3/4A, a NS3/4A protein expression vector, followed by treatment with 10 μM andrographolide in the absence or presence of SnPP for 3 days. As a positive control, plasmid-transfected cells were treated with the specific NS3/4A inhibitor telaprevir at an effective concentration of 1 μM. As shown in Figure 5B, andrographolide concentration-dependently inhibited NS3/4A protease activity, and this inhibitory effect was concentration-dependently attenuated by SnPP (Figure 5C). To confirm that the increase in HO-1 contributes to the anti-HCV activity of andrographolide, we used SnPP and HO-1 shRNA for evaluating the inhibitory effect of andrographolide on HCV replication. Ava5 cells were incubated with increasing concentrations of SnPP in the presence of 10 μM andrographolide for 3 days. As shown in Figure 6A, SnPP concentration- dependently attenuated the andrographolide-induced reduction in HCV protein synthesis (lanes 2–6) compared with no treatment (lane 1). qRT-PCR provided similar results for HCV RNA levels under the same experimental conditions described earlier (Figure 6B).

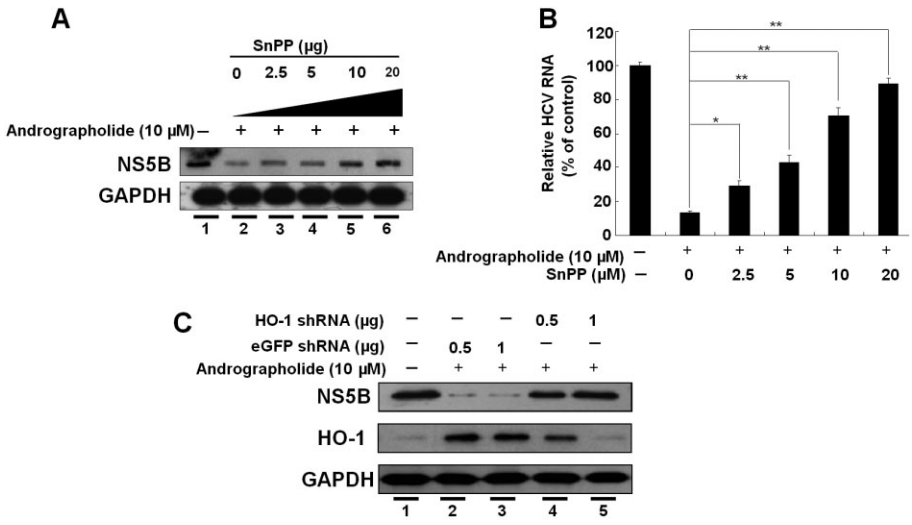

Figure 6

Inhibition of HO-1 expression attenuates the suppression of HCV replication by andrographolide. (A, B) Restoration of andrographolide-reduced HCV protein synthesis (A) and HCV RNA replication (B) by the HO-1-specific inhibitor SnPP. Ava5 cells were co-incubated with andrographolide (10 μM) and increasing concentrations of SnPP (0–20 μM) for 3 days. The cell lysates and total RNAs were subjected to Western blotting and qRT-PCR analysis respectively. The HCV RNA level was normalized against the cellular *gapdh* mRNA level and presented as the % change relative to andrographolide/SnPP-untreated cells (defined as 100%). (C) Restoration of andrographolide-reduced HCV protein synthesis by HO-1 gene knockdown. Ava5 cells were transfected with non-specific eGFP shRNA vectors or different amounts of the HO-1-specific shRNA (0.5 and 1.0 μg) for 12 h. The transfected cells were then treated with 10 μM andrographolide for 3 days. Protein synthesis was detected by Western blotting with anti-HCV NS5B or anti-HO-1 antibody. Equal loading of cell lysates was confirmed by probing the same blot with anti-GAPDH antibody. The experiments were performed in triplicate, and error bars indicate mean ± SD. *$P < 0.05$, **$P < 0.01$.

Silencing HO-1 by shRNA transfection also reduced the inhibitory effect of andrographolide on HCV protein synthesis in the Ava5 cells (Figure 6C, lanes 4 and 5) compared with non-targeted control eGFP shRNA transfection (Figure 6C, lanes 2 and 3). Of note, the andrographolide-reduced HCV protein levels were almost restored to those in the untreated Ava5 cells when HO-1 expression was effectively silenced (Figure 6C, lanes 1 and 5). Collectively, these results indicate that the increase in HO-1 induced by andrographolide contributes to its anti-HCV activity by increasing the IFN response and suppressing HCV NS3/4A protease activity.

Anti-HCV activity of andrographolide is correlated with an Nrf2-mediated increase in HO-1

Nrf2 functions as an important upstream regulator in the mediation of HO-1 expression. To determine whether andrographolide-induced HO-1 increase is mediated by Nrf2 activation, Nrf2 nuclear translocation and Nef2-mediated ARE activation for HO-1 expression were examined. Ava5 cells were treated with andrographolide for 3 days, followed by Western blotting. As shown in Figure 7A, andrographolide concentration-dependently increased the total amount of cellular and nuclear Nrf2 protein. At a concentration of andrographolide (10 μM) shown to have anti-HCV activity, nuclear Nrf2 protein levels gradually accumulated in a time-dependent manner (Figure 7B). As expected, ARE-driven firefly luciferase activity was concentration-dependently increased by andrographolide (Figure 7C). In contrast, inhibition of Nrf2 expression by shRNA-mediated gene silencing simultaneously suppressed the andrographolide-induced increased HO-1 expression and attenuated the anti-HCV activity of andrographolide (Figure 7D, lanes 4 and 5) compared with no treatment (lane 1) and non-specific eGFP shRNA transfection of andrographolide-treated Ava5 cells (lanes 2 and 3). Given that the activation of Nrf2 nuclear translocation is regulated by Keap1-dependent ubiquitination (Kwak *et al.*, 2004), we next investigated the effect of andrographolide on Keap1 expression by Western blotting. No significant change in Keap1 protein levels was observed in the presence of andrographolide, at increasing concentrations for 3 days (Figure 7E, upper panel). Bach1, a negative regulator of HO-1 induction, functions as a competitor of Nrf2 for binding to ARE in the HO-1 promoter region (Kaspar and Jaiswal, 2010). Bach1 expression was next examined, and no significant change in Bach1 protein levels was observed under the same experimental conditions (Figure 7E, middle panel). Collectively, these results indicated that the Nrf2–ARE signalling pathway is strongly associated with the mechanism of Nrf2-mediated HO-1 increase responsible for the anti-HCV activity of andrographolide and, therefore, the upstream regulation of Nrf2 activation by andrographolide should be further investigated.

p38 MAPK is involved in Nrf2-mediated HO-1 increase induced by andrographolide

Activation of MAPK signalling cascades including p38 MAPK, ERK1/2 and JNK has been reported to increase HO-1 gene expression and anti-HCV activity (Huang *et al.*, 2006; Yano *et al.*, 2009; Pei *et al.*, 2012). To investigate the involvement

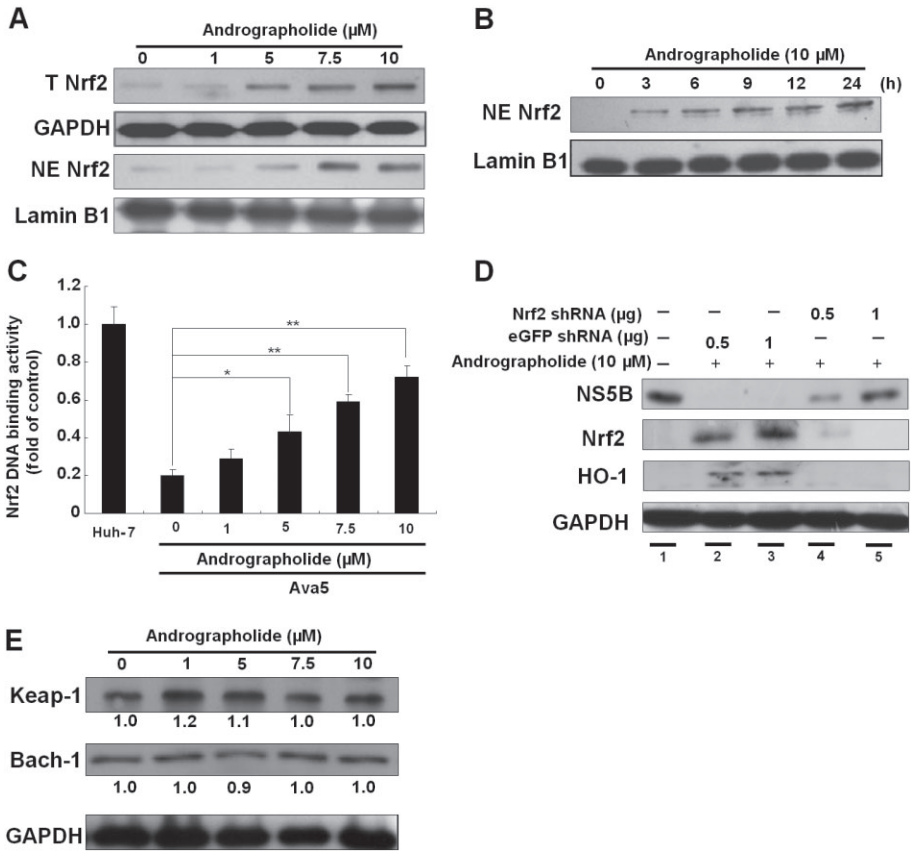

Figure 7

Andrographolide induces Nrf2 expression in Ava5 cells. (A–C) Induction of Nrf2 expression (A), Nrf2 nuclear translocation (B) and Nrf2-mediated ARE transactivation (C) by andrographolide in a concentration- or time-dependent manner. Ava5 or p2xARE-Luc-transfected Ava5 cells were treated with andrographolide at the indicated concentrations (0–10 μM) for 3 days. Each transfection mixture contained 0.1 μg pSEAP reporter plasmid as a control of transfection efficiency. The cytoplasmic and nuclear fractions of cell lysates were assayed by Western blotting with anti-Nrf2, anti-lamin B or anti-GAPDH (loading control) antibody. Nrf2 nuclear translocation was examined at different time points (0–24 h) after incubation with 10 μM andrographolide. Nrf2-mediated ARE transactivation was determined by luciferase activity following normalization against SEAP activity and presented as fold activation relative to the basal levels of ARE transactivation activity in parental Huh-7 cells (defined as 1). (D) Restoration of andrographolide-reduced HCV protein synthesis by Nrf2 gene knockdown. Ava5 cells were transfected with non-specific eGFP shRNA or different amounts of the Nrf2-specific shRNA (0.5 and 1 μg) vectors for 12 h. Then, the transfected cells were treated with 10 μM andrographolide for 3 days. Protein synthesis was assayed by Western blotting with anti-NS5B, anti-Nrf2 or anti-HO-1 antibody. Equal loading of cell lysates was confirmed by probing the same blot with anti-GAPDH antibody. (E) Andrographolide had no significant effect on Keap1 and Bach1 expression. Ava5 cells were treated with andrographolide at the indicated concentrations (0–10 μM) for 3 days. The Keap1 and Bach1 protein levels were assayed by Western blotting with anti-Keap1 and anti-Bach1 antibodies respectively. Equal loading of cell lysates was confirmed by probing the same blot with anti-GAPDH antibody. Band intensity was quantified by densitometric scanning and presented as fold value relative to the andrographolide-untreated control (defined as 1) following normalization against the GAPDH protein level. The experiments were performed in triplicate, and error bars indicate mean ± SD. $*P < 0.05$, $**P < 0.01$.

of MAPKs in the anti-HCV activity of andrographolide, the phosphorylation status of the three MAPK molecules was first assayed by Western blotting with phospho-specific antibodies. Ava5 cells were treated with 10 μM andrographolide for 0–120 min. As shown in Figure 8A, phospho-38 MAPK protein levels were time- dependently elevated by andrographolide treatment in comparison with the time point of 0 min. In contrast, andrographolide showed no significant effect on ERK1/2 or JNK phosphorylation at any time point. In order to clarify the role of p38 MAPK in the Nrf2-mediated HO-1 increase, which mediates the anti-HCV activity of andrographolide, we investigated the effects of specific inhibitors against ERK1/2 (PD98059), JNK (SP600125) and p38 MAPK (SB203580) on the protein levels of Nrf2, HO-1 and HCV. As shown in Figure 8B, Western blotting revealed that the andrographolide-elevated protein levels of HO-1, total Nrf2 and nuclear Nrf2 were significantly reduced by the p38 MAPK inhibitor (lane 4) but not by the ERK1/2 (lane 3) or the JNK (lane 5) inhibitor. Of note, the p38 MAPK inhibitor reversed the andrographolide-induced reduction in HCV protein synthesis (lane 4) compared with the non-drug treated control (lane 1) or andrographolide treatment alone (lane 2), whereas the ERK1/2 or JNK inhibitor showed no obvious effect on the Nrf2 and HO-1 protein levels under the same experimental conditions (lanes 3 and 5). Also, the suppressive effect of andrographolide on HCV protein synthesis

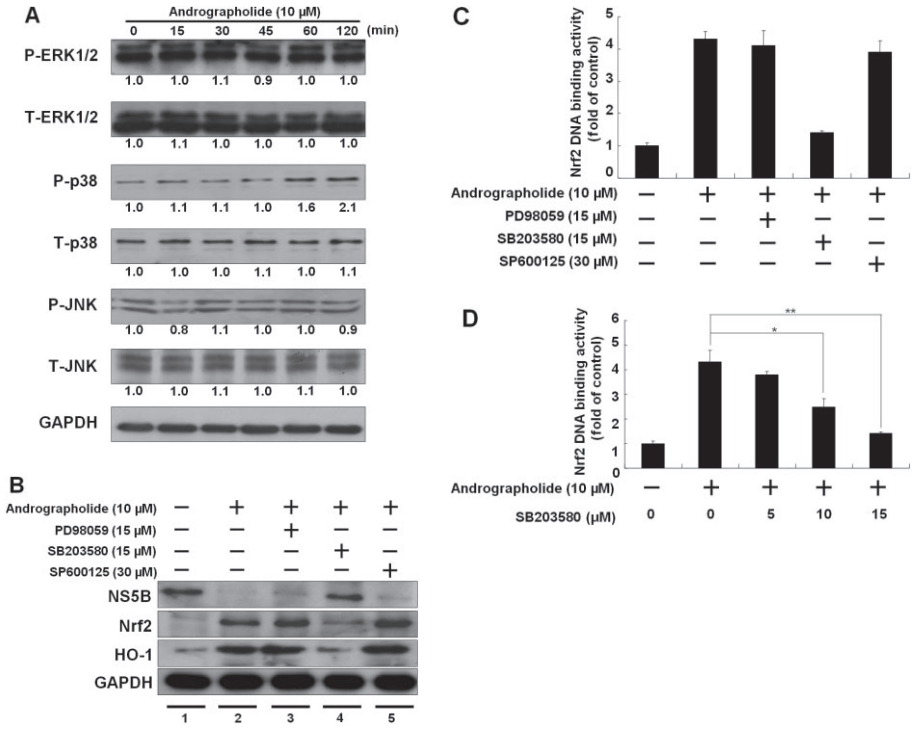

Figure 8

Andrographolide activates p38 MAPK phosphorylation to stimulate the Nrf2–HO-1 signalling pathway for anti-HCV activity. (A) Andrographolide activated p38 MAPK phosphorylation in a time-dependent manner. Ava5 cells were treated with 10 μM andrographolide at the indicated time points (0–120 min), and total protein was assayed by Western blotting with anti-phospho-ERK1/2, anti-ERK1/2, anti-phospho-p38, anti-p38, anti-phospho-JNK, anti-JNK and anti-GAPDH (loading control) antibodies. Band intensity was quantified by densitometric scanning and presented as fold value relative to the time point of 0 min (defined as 1) following normalization against the GAPDH protein level. (B) Restoration of andrographolide-reduced HCV protein synthesis by p38 MAPK inhibitor. Ava5 cells were co-treated with 10 μM andrographolide and each MAPK molecule inhibitor against the ERK (PD98059), p38 (SB203580) or JNK inhibitor (SP600125) at the indicated concentration for 3 days. The cell lysates were assayed by Western blotting with anti-NS5B, anti-Nrf2, anti-HO-1 or anti-GAPDH antibody. Equal loading of cell lysates was confirmed by the GAPDH protein level. (C) The andrographolide-induced Nrf2 transactivation was restored to control levels by the p38 MAPK inhibitor SB203580. The cell lysates of p2xARE-Luc-transfected Ava5 cells were analysed for luciferase activity under the experimental conditions described earlier. Each transfection mixture contained 0.1 μg pSEAP reporter plasmid as a control of transfection efficiency. Nrf2-mediated ARE transactivation was assayed for luciferase activity and presented as fold activation relative to drug-untreated cells (defined as 1) following normalization against SEAP activity. (D) The p38 MAPK inhibitor suppressed the andrographolide-induced Nrf2 transactivation in a concentration-dependent manner. The cell lysates of p2xARE-Luc-transfected Ava5 cells were assayed for luciferase activity in the presence of 10 μM andrographolide with increasing concentrations of the p38 MAPK inhibitor SB203580 (0–15 μM) for 3 days. The luciferase activity was presented as fold change relative to andrographolide/SB203580-untreated cells (defined as 1) following normalization against SEAP activity. The experiments were performed in triplicate, and error bars indicate mean ± SD. *$P < 0.05$, **$P < 0.01$.

was not restored by either the ERK1/2 or JNK inhibitor. Furthermore, the p38 MAPK, but not the ERK1/2 or JNK, inhibitor concentration- dependently abolished the elevated Nrf2/ARE-driven luciferase activity induced by andrographolide (Figure 8C and D). These results suggest that the anti-HCV activity of andrographolide is associated with a p38 MAPK/Nrf2-mediated up-regulation of HO-1 expression in hepatoma cells.

Andrographolide combined with IFN-α or viral target inhibitors synergistically inhibits HCV replication

To determine whether combining andrographolide with other anti-HCV drugs, including IFN-α, the NS3/4A inhibitor telaprevir (Forestier and Zeuzem, 2012) and NS5B inhibitor PSI-7977 (Lam *et al.*, 2012), can enhance anti-HCV activity, Ava5 cells were treated with andrographolide in combination with each of the specific inhibitors at various concentration ratios for 3 days. The effects were evaluated by computer modelling, as described by Chou and Talalay (1984). We first assessed the effect of andrographolide on the anti-HCV EC_{90} values for the anti-HCV drugs. For each combination studied, andrographolide was effective at decreasing the EC_{90} value of each tested drug 0.33–0.67-fold at different concentrations, when compared with the no andrographolide control (Supporting Information Figure S1). A synergistic effect was further identified, as is evident from the CI values ranging from 0.65 to 0.81 for EC_{50}, EC_{75} and EC_{90} respectively (Table 2). No significant drug cytotoxicity was observed for any treatment combination, as assessed by a colorimetric MTS assay (data not shown). Taken together, these results

Table 2

Anti-HCV activity of andrographolide combination studies with IFN-α and other viral enzyme inhibitors

Combination compound	CI values at EC_{50}	EC_{75}	EC_{90}	Influence
IFN-α	0.78 ± 0.015	0.75 ± 0.024	0.73 ± 0.052	Synergistic
Telaprevir	0.72 ± 0.07	0.79 ± 0.035	0.81 ± 0.02	Synergistic
PSI-7977	0.65 ± 0.05	0.69 ± 0.043	0.75 ± 0.022	Synergistic

Ava5 cells were treated with various concentration ratios of andrographolide and each inhibitor targeting NS3/4A protease (telaprevir) or NS5B polymerase (PSI-7977) for 3 days. The tested concentrations are described in Methods section. qRT-PCR was used to determine anti-HCV activity. Combination index (CI) values at effective concentration achieving 50% (EC_{50}), 75% (EC_{75}) and 90% (EC_{90}) inhibition were calculated using CalcuSyn software. As defined by the CalcuSyn program, CI < 1, CI = 1 and CI > 1 indicate synergism, additive effect and antagonism respectively.

suggest that andrographolide may serve as a dietary/herbal supplement for enhancing therapeutic effects in combating HCV infection.

Discussion and conclusion

In this study, our data clearly demonstrated that andrographolide strongly up-regulated HO-1 RNA and protein levels, resulting in the accumulation of its metabolite biliverdin for efficient suppression of HCV RNA replication (Figures 1–3). Our results are consistent with the recent findings of Lehmann *et al*. and Zhu *et al*. showing that biliverdin from HO-1 protects against virus infection by enhancement of the antiviral IFN response and inhibition of HCV NS3/4A protease activity (Figures 4 and 5). These antiviral effects of andrographolide were abolished by the selective HO-1 inhibitor SnPP or specific shRNA silencing (Figure 6). We also confirmed that Nrf-2-mediated HO-1 induction contributed to anti-HCV activity of andrographolide by Nrf2 knockdown (Figure 7D). In contrast, we detected no change in Keap1 and Bach1 expression following exposure to andrographolide (Figure 7E). Moreover, we found that the Nrf-2-mediated increase in HO-1 induced by andrographolide was associated with p38 MAPK activity (Figure 8). On the basis of the findings presented here, we propose a model to demonstrate the action of andrographolide against HCV infection. As shown in Figure 9, activation of the p38 MAPK signalling pathway by andrographolide is required for the the accumulation of Nrf2, which then increases the expression of HO-1 that then produces biliverdin, which inhibits HCV replication by increasing the antiviral IFN responses and suppressing HCV NS3/4A protease activity. Numerous studies have demonstrated that andrographolide possesses an anti-inflammatory effect via inactivation of NF-κB (Bao *et al*., 2009; Chen *et al*., 2011; Lim *et al*., 2012; Zhu *et al*., 2013). Based on earlier findings that showed potential anti-HCV agents prevent the replication of HCV by suppressing NF-κB-mediated COX-2 (Lee *et al*., 2011a,b; Chen *et al*., 2013a; Lin *et al*., 2013), we propose that the inhibitory effect of andrographolide on NF-κB might in part contribute to its anti-HCV activity. This hypothesis should be investigated in the future. In addition to the effect of upstream kinase p38 MAPK, Nrf2/ARE-mediated HO-1 expression can be regulated by other enzymes, such as PKC, PI3K, Akt and glycogen synthase kinase 3 beta, for the maintenance of cellular redox homeostasis against different stress (Paine *et al*., 2010). Further studies are needed to elucidate any additional signalling pathways involved in the anti-HCV activity of andrographolide.

HO-1 up-regulation as a host defence mechanism against viral replication has been observed with other viruses, such as HIV (Devadas *et al*., 2010) and spring viraemia of carp virus (Yuan *et al*., 2012). Indeed, we have recently shown that a phytocompound, lucidone, increases HO-1 and has significant anti-HCV activity (Chen *et al*., 2013b). Apart from its antiviral action, an up-regulation of HO-1 has been reported to be associated with cytoprotection in chronic hepatic inflammation mediated by its reaction products (Sass *et al*., 2012). Chronic inflammation caused by HCV infection has been suggested to be a risk factor associated with the development of cirrhosis and HCC (Buhler and Bartenschlager, 2012). It is thus desirable to further investigate the inhibitory effect of andrographolide on HCV-induced inflammation. Recent studies have demonstrated that andrographolide can induce autophagic cell death in human liver cancer cells at high concentrations (Chen *et al*., 2012), indicating that andrographolide administration may be of benefit in therapeutic strategies for HCV-associated liver diseases.

In addition to telaprevir and boceprevir, the first FDA-approved (in 2011) HCV protease inhibitors, many new drugs targeting specific viral proteins are in development and clinical trials (Soriano *et al*., 2011). However, drug resistance is a major challenge when treating HCV infection because of the low fidelity of HCV polymerase during viral replication. For this reason, targeting host proteins against viral infection may be a promising strategy to prevent resistance emergence, given that the mutation rate of the host genome is lower than that of the RNA virus genome, and combinations of drugs with different targets may increase the response rate and decrease the risk of resistance emerging (Sanjuan *et al*., 2010). Drug combination therapy is also a promising approach to increase therapeutic efficacy and decrease potential toxicity in comparison with mono-drug therapy. Accordingly, andrographolide can be considered as a suitable candidate for HCV therapy that minimizes the risk of drug resistance by targeting host HO-1 expression and synergistically inhibiting HCV

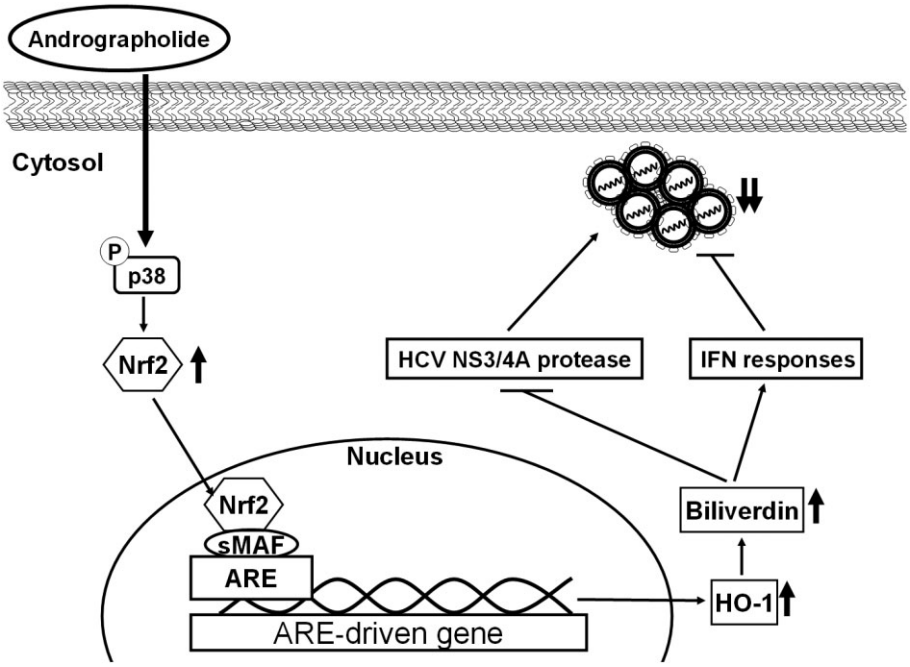

Figure 9

Model describing the inhibition of HCV replication by andrographolide. Andrographolide induces p38 MAPK activation and subsequently increases Nrf2-mediated HO-1 expression, leading to the generation of biliverdin against HCV replication by enhancement of antiviral IFN responses and inhibition of HCV NS3/4A protease activity.

replication in combination with inhibitors against different targets (Table 2). Further studies are warranted to clarify the potential clinical relevance of our findings.

In summary, our results show that andrographolide treatment markedly reduced HCV replication and exerted a synergistic effect on anti-HCV activity in combination with current drugs, IFN-α and telaprevir, or the clinical trial drug PSI-7977. These results indicate that andrographolide may be considered as a dietary supplement or potential drug for the treatment of patients with HCV. Our results shed light on the anti-HCV mechanism of andrographolide, which was shown to involve the induction of the p38 MAPK/Nrf2/HO-1 pathway; this may represent a therapeutic target for future development and discovery of anti-HCV drugs.

Acknowledgements

We thank Dr. Anupam Agarwal (University of Alabama, AL, USA) and Dr. Being-Sun Wung (National Chiayi University, Taiwan) for kindly providing pHOGL3/9.4 and p2xARE-Luc plasmids respectively. We are grateful to Dr. Charles Rice (Rockefeller University and Apath, LLC, NY, USA) for kindly supporting human hepatoma cell line (Huh-7 and Huh-7.5) and hepatitis C virus replicon cell line Ava5. We also thank T. Wakita (National Institute of Infectious Diseases, Japan) for providing HCVcc plasmid. This work was supported by a grant from the National Science Council of Taiwan (NSC 97-2311-B-037-001-MY3) and in part by a grant from the National Sun Yat-Sen University-KMU Joint Research Project (NSYSU-KMU 102-I004).

Conflict of interest

None.

References

Alter MJ (2007). Epidemiology of hepatitis C virus infection. World J Gastroenterol 13: 2436–2441.

Bao Z, Guan S, Cheng C, Wu S, Wong SH, Kemeny DM *et al.* (2009). A novel antiinflammatory role for andrographolide in asthma via inhibition of the nuclear factor-kappaB pathway. Am J Respir Crit Care Med 179: 657–665.

Blight KJ, Kolykhalov AA, Rice CM (2000). Efficient initiation of HCV RNA replication in cell culture. Science 290: 1972–1974.

Brass V, Moradpour D, Blum HE (2006). Molecular virology of hepatitis C virus (HCV): 2006 update. Int J Med Sci 3: 29–34.

Buhler S, Bartenschlager R (2012). Promotion of hepatocellular carcinoma by hepatitis C virus. Dig Dis 30: 445–452.

Chan SJ, Wong WS, Wong PT, Bian JS (2010). Neuroprotective effects of andrographolide in a rat model of permanent cerebral ischaemia. Br J Pharmacol 161: 668–679.

Chao CY, Lii CK, Hsu YT, Lu CY, Liu KL, Li CC *et al.* (2013). Induction of heme oxygenase-1 and inhibition of TPA-induced matrix metalloproteinase-9 expression by andrographolide in MCF-7 human breast cancer cells. Carcinogenesis 34: 1843–1851.

Chen HW, Lin AH, Chu HC, Li CC, Tsai CW, Chao CY *et al.* (2011). Inhibition of TNF-α-induced inflammation by andrographolide via down-regulation of the PI3K/Akt signaling pathway. J Nat Prod 74: 2408–2413.

Chen JX, Xue HJ, Ye WC, Fang BH, Liu YH, Yuan SH *et al.* (2009). Activity of andrographolide and its derivatives against influenza virus *in vivo* and *in vitro*. Biol Pharm Bull 32: 1385–1391.

Chen KJ, Tseng CK, Chang FR, Yang JI, Yeh CC, Chen WC *et al.* (2013a). Aqueous extract of the edible *Gracilaria tenuistipitata* inhibits hepatitis C viral replication via cyclooxygenase-2 suppression and reduces virus-induced inflammation. PLoS ONE 8: e57704.

Chen W, Feng L, Nie H, Zheng X (2012). Andrographolide induces autophagic cell death in human liver cancer cells through cyclophilin D-mediated mitochondrial permeability transition pore. Carcinogenesis 33: 2190–2198.

Chen WC, Wang SY, Chiu CC, Tseng CK, Lin CK, Wang HC *et al.* (2013b). Lucidone suppresses hepatitis C virus replication by Nrf2-mediated heme oxygenase-1 induction. Antimicrob Agents Chemother 57: 1180–1191.

Chou TC, Talalay P (1984). Quantitative analysis of dose–effect relationships: the combined effects of multiple drugs or enzyme inhibitors. Adv Enzyme Regul 22: 27–55.

Coon JT, Ernst E (2004). *Andrographis paniculata* in the treatment of upper respiratory tract infections: a systematic review of safety and efficacy. Planta Med 70: 293–298.

Devadas K, Hewlett IK, Dhawan S (2010). Lipopolysaccharide suppresses HIV-1 replication in human monocytes by protein kinase C-dependent heme oxygenase-1 induction. J Leukoc Biol 87: 915–924.

Farombi EO, Surh YJ (2006). Heme oxygenase-1 as a potential therapeutic target for hepatoprotection. J Biochem Mol Biol 39: 479–491.

Forestier N, Zeuzem S (2012). Telaprevir for the treatment of hepatitis C. Expert Opin Pharmacother 13: 593–606.

Ghany MG, Strader DB, Thomas DL, Seeff LB (2009). Diagnosis, management, and treatment of hepatitis C: an update. Hepatology 49: 1335–1374.

Guan SP, Tee W, Ng DS, Chan TK, Peh HY, Ho WE *et al.* (2013). Andrographolide protects against cigarette smoke-induced oxidative lung injury via augmentation of Nrf2 activity. Br J Pharmacol 168: 1707–1718.

Hill-Kapturczak N, Sikorski E, Voakes C, Garcia J, Nick HS, Agarwal A (2003). An internal enhancer regulates heme- and cadmium-mediated induction of human heme oxygenase-1. Am J Physiol Renal Physiol 285: F515–F523.

Huang Y, Chen XC, Konduri M, Fomina N, Lu J, Jin L *et al.* (2006). Mechanistic link between the anti-HCV effect of interferon gamma and control of viral replication by a Ras-MAPK signaling cascade. Hepatology 43: 81–90.

Kaspar JW, Jaiswal AK (2010). Antioxidant-induced phosphorylation of tyrosine 486 leads to rapid nuclear export of Bach1 that allows Nrf2 to bind to the antioxidant response element and activate defensive gene expression. J Biol Chem 285: 153–162.

Kato T, Matsumura T, Heller T, Saito S, Sapp RK, Murthy K *et al.* (2007). Production of infectious hepatitis C virus of various genotypes in cell cultures. J Virol 81: 4405–4411.

Kiser JJ, Burton JR, Anderson PL, Everson GT (2012). Review and management of drug interactions with boceprevir and telaprevir. Hepatology 55: 1620–1628.

Kravets A, Hu Z, Miralem T, Torno MD, Maines MD (2004). Biliverdin reductase, a novel regulator for induction of activating transcription factor-2 and heme oxygenase-1. J Biol Chem 279: 19916–19923.

Kwak MK, Wakabayashi N, Kensler TW (2004). Chemoprevention through the Keap1-Nrf2 signaling pathway by phase 2 enzyme inducers. Mutat Res 555: 133–148.

Lam AM, Espiritu C, Bansal S, Micolochick Steuer HM, Niu C, Zennou V *et al.* (2012). Genotype and subtype profiling of PSI-7977 as a nucleotide inhibitor of hepatitis C virus. Antimicrob Agents Chemother 56: 3359–3368.

Lee JC, Shih YF, Hsu SP, Chang TY, Chen LH, Hsu JT (2003). Development of a cell-based assay for monitoring specific hepatitis C virus NS3/4A protease activity in mammalian cells. Anal Biochem 316: 162–170.

Lee JC, Tseng CK, Chen KJ, Huang KJ, Lin CK, Lin YT (2010). A cell-based reporter assay for inhibitor screening of hepatitis C virus RNA-dependent RNA polymerase. Anal Biochem 403: 52–62.

Lee JC, Chen WC, Wu SF, Tseng CK, Chiou CY, Chang FR *et al.* (2011a). Anti-hepatitis C virus activity of *Acacia confusa* extract via suppressing cyclooxygenase-2. Antiviral Res 89: 35–42.

Lee JC, Tseng CK, Wu SF, Chang FR, Chiu CC, Wu YC (2011b). San-Huang-Xie-Xin-Tang extract suppresses hepatitis C virus replication and virus-induced cyclooxygenase-2 expression. J Viral Hepat 18: e315–e324.

Lehmann E, El-Tantawy WH, Ocker M, Bartenschlager R, Lohmann V, Hashemolhosseini S *et al.* (2010). The heme oxygenase 1 product biliverdin interferes with hepatitis C virus replication by increasing antiviral interferon response. Hepatology 51: 398–404.

Liang L, Gao C, Luo M, Wang W, Zhao C, Zu Y *et al.* (2013). Dihydroquercetin (DHQ) induced HO-1 and NQO1 expression against oxidative stress through the Nrf2-dependent antioxidant pathway. J Agric Food Chem 61: 2755–2761.

Liao BC, Hsieh CW, Liu YC, Tzeng TT, Sun YW, Wung BS (2008). Cinnamaldehyde inhibits the tumor necrosis factor-alpha-induced expression of cell adhesion molecules in endothelial cells by suppressing NF-kappaB activation: effects upon IkappaB and Nrf2. Toxicol Appl Pharmacol 229: 161–171.

Lim JC, Chan TK, Ng DS, Sagineedu SR, Stanslas J, Wong WS (2012). Andrographolide and its analogues: versatile bioactive molecules for combating inflammation and cancer. Clin Exp Pharmacol Physiol 39: 300–310.

Lin TP, Chen SY, Duh PD, Chang LK, Liu YN (2008). Inhibition of the Epstein–Barr virus lytic cycle by andrographolide. Biol Pharm Bull 31: 2018–2023.

Lin YT, Wu YH, Tseng CK, Lin CK, Chen WC, Hsu YC *et al.* (2013). Green tea phenolic epicatechins inhibit hepatitis C virus replication via cycloxygenase-2 and attenuate virus-induced inflammation. PLoS ONE 8: e54466.

Maines MD (2005). The heme oxygenase system: update 2005. Antioxid Redox Signal 7: 1761–1766.

Maiti K, Mukherjee K, Murugan V, Saha BP, Mukherjee PK (2010). Enhancing bioavailability and hepatoprotective activity of andrographolide from *Andrographis paniculata*, a well-known medicinal food, through its herbosome. J Sci Food Agric 90: 43–51.

Onomoto K, Jogi M, Yoo JS, Narita R, Morimoto S, Takemura A *et al.* (2012). Critical role of an antiviral stress granule containing RIG-I and PKR in viral detection and innate immunity. PLoS ONE 7: e43031.

Paine A, Eiz-Vesper B, Blasczyk R, Immenschuh S (2010). Signaling to heme oxygenase-1 and its anti-inflammatory therapeutic potential. Biochem Pharmacol 80: 1895–1903.

Pei R, Zhang X, Xu S, Meng Z, Roggendorf M, Lu M *et al.* (2012). Regulation of hepatitis C virus replication and gene expression by the MAPK-ERK pathway. Virol Sin 27: 278–285.

Sanjuan R, Nebot MR, Chirico N, Mansky LM, Belshaw R (2010). Viral mutation rates. J Virol 84: 9733–9748.

Sarrazin C, Zeuzem S (2010). Resistance to direct antiviral agents in patients with hepatitis C virus infection. Gastroenterology 138: 447–462.

Sass G, Barikbin R, Tiegs G (2012). The multiple functions of heme oxygenase-1 in the liver. Z Gastroenterol 50: 34–40.

Schoggins JW, Wilson SJ, Panis M, Murphy MY, Jones CT, Bieniasz P *et al*. (2011). A diverse range of gene products are effectors of the type I interferon antiviral response. Nature 472: 481–485.

Seubsasana S, Pientong C, Ekalaksananan T, Thongchai S, Aromdee C (2011). A potential andrographolide analogue against the replication of herpes simplex virus type 1 in vero cells. Med Chem 7: 237–244.

Shan Y, Lambrecht RW, Donohue SE, Bonkovsky HL (2006). Role of Bach1 and Nrf2 in up-regulation of the heme oxygenase-1 gene by cobalt protoporphyrin. FASEB J 20: 2651–2653.

Soriano V, Vispo E, Poveda E, Labarga P, Martin-Carbonero L, Fernandez-Montero JV *et al*. (2011). Directly acting antivirals against hepatitis C virus. J Antimicrob Chemother 66: 1673–1686.

Sule A, Ahmed QU, Latip J, Samah OA, Omar MN, Umar A *et al*. (2012). Antifungal activity of *Andrographis paniculata* extracts and active principles against skin pathogenic fungal strains *in vitro*. Pharm Biol 50: 850–856.

Susser S, Welsch C, Wang Y, Zettler M, Domingues FS, Karey U *et al*. (2009). Characterization of resistance to the protease inhibitor boceprevir in hepatitis C virus-infected patients. Hepatology 50: 1709–1718.

Uttekar MM, Das T, Pawar RS, Bhandari B, Menon V *et al*. (2012). Anti-HIV activity of semisynthetic derivatives of andrographolide and computational study of HIV-1 gp120 protein binding. Eur J Med Chem 56: 368–374.

Yano M, Ikeda M, Abe K, Kawai Y, Kuroki M, Mori K *et al*. (2009). Oxidative stress induces anti-hepatitis C virus status via the activation of extracellular signal-regulated kinase. Hepatology 50: 678–688.

Yu AL, Lu CY, Wang TS, Tsai CW, Liu KL, Cheng YP *et al*. (2010). Induction of heme oxygenase 1 and inhibition of tumor necrosis factor alpha-induced intercellular adhesion molecule expression by andrographolide in EA.hy926 cells. J Agric Food Chem 58: 7641–7648.

Yuan J, Su N, Wang M, Xie P, Shi Z, Li L (2012). Down-regulation of heme oxygenase-1 by SVCV infection. Fish Shellfish Immunol 32: 301–306.

Zhu T, Wang DX, Zhang W, Liao XQ, Guan X, Bo H *et al*. (2013). Andrographolide protects against LPS-induced acute lung injury by inactivation of NF-kappaB. PLoS ONE 8: e56407.

Zhu Z, Wilson AT, Luxon BA, Brown KE, Mathahs MM, Bandyopadhyay S *et al*. (2010). Biliverdin inhibits hepatitis C virus nonstructural 3/4A protease activity: mechanism for the antiviral effects of heme oxygenase? Hepatology 52: 1897–1905.

Supporting information

Additional Supporting Information may be found in the online version of this article at the publisher's web-site:

http://dx.doi.org/10.1111/bph.12440

Figure S1 Changes in anti-HCV activity of IFN-α or other viral enzyme inhibitors in combination with andrographolide. According to the analysis of drug synergism described in Methods section, the antiviral efficacy of each anti-HCV drug in combination with andrographolide at 2.5, 5.0 or 7.5 μM was presented as the fold change in EC_{90} value relative to the andrographolide-untreated control (defined as 1). The experiments were performed in triplicate, and error bars indicate mean ± SD.